

Superfluid Transition of ^4He in Ultralight Aerogel

Jongsoo Yoon,* Dmitri Sergatskov,[†] Jian Ma,[‡] Norbert Mulders,[§] and Moses H. W. Chan

Department of Physics, Pennsylvania State University, University Park, Pennsylvania 16802

(Received 5 November 1997)

We present superfluid density and heat capacity results of ^4He entrained in 5%, 2%, and 0.5% dense silica aerogel. The superfluid density exponent shows a systematic decrease towards the bulk ^4He value with decreasing aerogel density. Singular contribution to heat capacity is observed on both sides of the transition in aerogel of 2% and 0.5% silica. In the lightest sample, the scaling law $\alpha = \alpha'$ and the hyperscaling relation $2 - \alpha = d\nu = d\zeta$ are satisfied. [S0031-9007(97)05256-3]

PACS numbers: 67.40.Kh, 67.40.Hf, 67.40.Yv

The critical behavior of the superfluid transition of ^4He entrained in aerogel has recently been studied [1–5] in samples where the silica network constitutes 6% to 9% of the total available volume. The highly ramified structure of aerogel is made up of silica strands of about 5 nm in diameter interconnected at random sites; the distance between neighboring strands ranges up to 200 nm [6,7]. In spite of the highly irregular environment, a very sharp transition is found [1–5]. The superfluid density vanishes at the same temperature where the heat capacity has its maximum, suggesting that we are observing a genuine phase transition. The superfluid density (ρ_s) vanishes according to a simple power law of the form

$$\rho_s(t) = \rho_{s0}|t|^\zeta. \quad (1)$$

t , the reduced temperature, is defined as $t = (T - T_c)/T_c$, where T_c is the transition temperature. The superfluid density exponent ζ is found to be 0.81 [2–4], significantly larger than the bulk value of 0.6705 found in pure ^4He [8]. In comparison, bulklike exponent, consistent with theoretical expectation [9,10], is found for ^4He in Vycor glass [2] and in porous gold [9].

The contrasting critical behavior (in aerogel vs in Vycor glass and in porous gold) is most likely related to the difference in the pore structure of these media, since it is known theoretically that correlated impurities can alter the critical behavior of the pure parent system [11]. A Monte Carlo simulation study, which mimics aerogel as a percolating cluster with fractal disorder, found a superfluid density exponent of 0.72, provided the helium correlation length does not exceed the fractal correlation length [12]. Small angle neutron scattering and electron microscopy of Vycor glass and porous gold show a dominant, characteristic length scale in the distribution of silica or gold, and, hence, also the pores [9,13,14]. There is no such characteristic length scale in aerogel. Small angle neutron and x-ray scattering found fractal-like correlations in the distribution of silica between 5 nm to typically 150 nm for aerogel of modest density (e.g., approximately 6% silica) [15]. The fractal regime is found to extend to larger length scales for lighter aerogels. At a length scale beyond the fractal-like regime, scattering data show a uniform distribution of the silica.

Attributing a nonbulklike exponent in aerogel to long range correlation of silica, however, is not entirely satisfactory because the behavior at very small t has not been explained. Simple power law dependence of ρ_s in 6% and 9% aerogel (i.e., with 6% or 9% volume fraction of silica) was found to extend inside $|t| = 10^{-4}$. If we assume the Josephson's relation [16,17] to be valid for ^4He in aerogel, namely,

$$\xi(t) = \xi_0|t|^{-\zeta} = \frac{k_B T_c m^2}{\hbar^2 \rho_s(t)}, \quad (2)$$

then the correlation length $\xi(t)$ in 6% aerogel is calculated to be 480 nm at $t = 10^{-4}$ [3]. In Eq. (2), m , k_B , and \hbar are, respectively, the mass of helium atoms, the Boltzmann's constant, and the Planck's constant. Since a length of 480 nm exceeds the upper limit of the fractal-like regime, one would expect ρ_s , in both 6% and 9% aerogel, to exhibit a crossover behavior such that the effective exponent ζ smoothly changes towards the bulk value when t is reduced from 10^{-2} towards 10^{-4} . Such a crossover is not seen.

Even more surprising are the results of the heat capacity measurements on 6% and 9% silica aerogel [3] and the thermal expansion coefficient (thermodynamically equivalent to heat capacity) measurements on 6% silica aerogel [5]. Whereas the data above T_c show singular behavior which can be described with a heat capacity exponent of $\alpha = -0.6$, the data below T_c show no singular contribution and they show essentially a linear dependence on T . This implies α' is close to -1 . If the values of α and α' are taken seriously, it would mean a violation of the scaling law $\alpha = \alpha'$. If the data were analyzed by imposing the condition $\alpha = \alpha'$, a value of -0.59 is found and, not surprisingly, the ratio A'/A is found to be indistinguishable from zero [5] (A' and A are, respectively, the amplitude of the singular heat capacity below and above T_c). In pure ^4He , A'/A is found to be 0.93 [18]. The values of α (-0.59) and ζ (0.81) are not consistent with the hyperscaling relation $d\nu = d\zeta = 2 - \alpha$ [16].

The effect of 6% and 9% silica on the critical behavior of superfluid ^4He in aerogel is both dramatic and puzzling. The aim of this study is to determine how the striking behavior evolves when the volume fraction of silica in

aerogel is reduced towards zero. We find that the singular contribution to the heat capacity, which is absent below T_c in 6% and 9% aerogel, shows up prominently in 2% and 0.5% aerogel. Both the superfluid density and heat capacity exponents show a smooth evolution towards the bulk values with reducing aerogel density. In 0.5% aerogel, the scaling law $\alpha = \alpha'$ and the hyperscaling relation are recovered.

The aerogel samples I (5% silica) and III (2% silica) used in ρ_s measurements were grown into a thin wall stainless steel cup by a two step base-catalyzed gelation process [6,7]. These cups were then attached to thin Be-Cu torsion rods and sealed, forming the bob of the torsional oscillator. Three aerogel samples, II (5% silica), IV (2% silica), and V (0.5% silica), were used for heat capacity studies. The aerogel of these samples was grown in the interstices of sintered silver grains of 100 μm in diameter. The packing ratio of the sintered silver is 60%. Silver sinter is used to achieve fast internal thermal equilibrium time for convenience and high precision heat capacity determinations. These aerogel samples were grown in our laboratory following the same process as that for samples I and III. Our attempt to make torsional oscillator measurements on a 0.5% aerogel sample, due to the extreme mechanical "softness" of the aerogel, was not successful. Therefore, torsional oscillator measurements in 0.5% aerogel were carried out on sample V (grown in sintered silver) after the heat capacity study was completed.

The superfluid density of ^4He in 5%, 2%, and 0.5% aerogel samples near their respective T_c are shown in Fig. 1. Even with the reinforcement of the sintered silver, the scatter in the data in the 0.5% sample is worse than those in

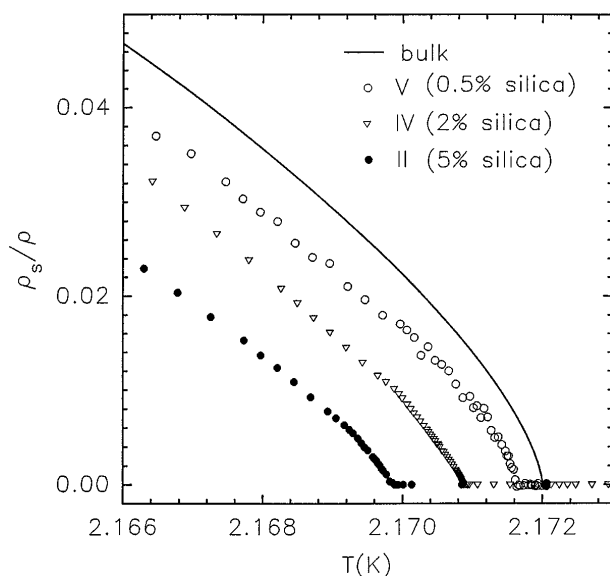


FIG. 1. The superfluid density near the superfluid transition of ^4He entrained in 5%, 2%, and 0.5% dense silica aerogel. The bulk data are from Ref. [8]. The transition temperatures are found to be $2.16985 \pm 3 \times 10^{-5}$ K, $2.17078 \pm 7 \times 10^{-5}$ K, and $2.1717 \pm 1 \times 10^{-4}$ K for ^4He in 5%, 2%, and 0.5% aerogel, respectively.

the other two samples. The superfluid transitions of all of the samples are very sharp, and, as expected, the transition temperature approaches the bulk value with decreasing silica volume fraction. With a λ point detector, T_λ can be located to within 5 μK , providing a fixed point for the temperature scale.

The superfluid density data are analyzed according to Eq. (1), using T_c , ρ_{so} , and ζ as free parameters in a non-linear least square fitting procedure. Our analysis of the data in the range $10^{-4} < |t| < 10^{-2}$ gives $\zeta = 0.79 \pm 0.01$ (33) for sample I (5% silica), 0.76 ± 0.01 (48) for sample III (2% silica), and 0.72 ± 0.015 (50) for sample V (0.05% silica). The data in the range $10^{-4} < |t| < 2 \times 10^{-3}$ yield $\zeta = 0.80 \pm 0.01$ (20), 0.78 ± 0.01 (34), and 0.71 ± 0.02 (30) for samples I, III, and V, respectively. The numbers in parentheses after the best fit values of ζ are the number of data points in the respective temperature ranges. The fact that the value of ζ is insensitive to the reduced temperature range of the data included in the analysis indicates that the simple power law as shown in Fig. 2 provides an excellent description of ρ_s near T_c and that there is no evidence of a crossover to a bulklike behavior even as $|t|$ approaches 10^{-4} . The value of ζ for 5% aerogel is in good agreement with that found for 6% and 9% aerogel [2-4]. Instead of a crossover with respect to $|t|$, the exponents in the three samples in this study show a clear trend towards the bulk value as the volume fraction of silica in aerogel is reduced.

Small angle x-ray scattering (SAXS) measurements were made on aerogels with 1.5%, 1%, and 0.5% silica grown in our laboratory [19]. Whereas the fractal-like regime in 1.5% aerogel extends up to 100 nm, in 0.5% aerogel it appears to extend to well beyond 200 nm, where the data stop. Smooth extrapolation of the data implies

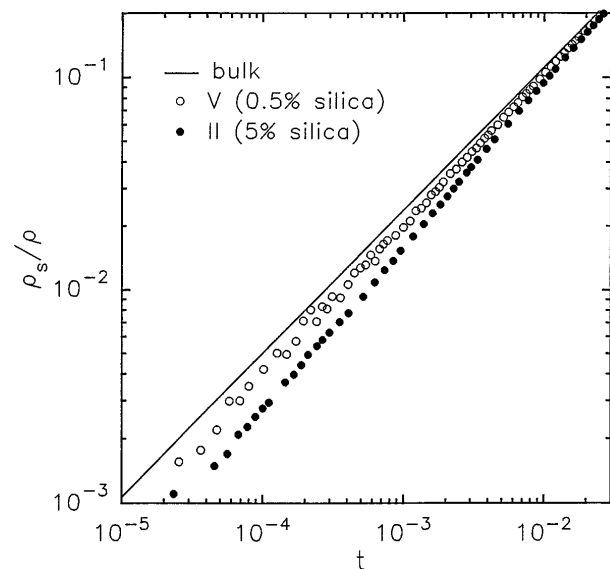


FIG. 2. Log-log plots for the superfluid density as a function of reduced temperature for bulk ^4He and for ^4He in 0.5% and 5% aerogel. The data for 2% aerogel would lie between that of 0.5% and 5% aerogel.

a length scale of the order of $1 \mu\text{m}$ to be the upper limit of the fractal-like regime, exceeding the correlation length of 220 nm at $|t| = 10^{-4}$. The correlation length is calculated from Eq. (2) using the value of ζ given above. This is in contrast to the case of 5% aerogel, where the correlation length of 320 nm at $|t| = 10^{-4}$ is beyond the fractal-like regime.

The heat capacity of ^4He in aerogel samples with 5%, 2%, and 0.5% silica near the superfluid transition are shown in Fig. 3. For comparison, the heat capacity of bulk ^4He , ^4He in 6% aerogel [3], and ^4He in porous gold [9] are also shown. The heat capacity is normalized by the coarse-grain-averaged volume of the entire experimental cell, which includes both the solid structure of aerogel and liquid helium contained therein. The heat capacity is measured by an ac technique [9,20]. The amount of sinusoidal heat at 0.1 Hz was adjusted so that the peak to peak temperature oscillation is about $100 \mu\text{K}$ near the heat capacity maximum. A small amount of bulk liquid (about 5%) was found in all three heat capacity cells. The presence of the bulk signal at T_λ provides a convenient fixed point in the temperature scale. The “scatters” near T_λ in Fig. 3 are due to imperfect subtraction of the bulk contribution.

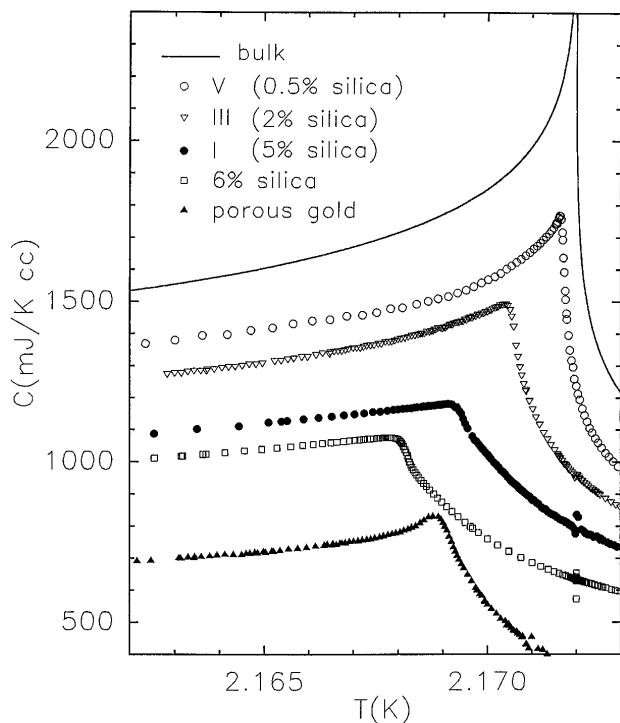


FIG. 3. The heat capacity near the superfluid transition of ^4He in aerogel with 0.5%, 2%, and 5% silica. The data for bulk ^4He (solid line, from Ref. [18]), ^4He in 6% aerogel (Ref. [3]), and ^4He in porous gold (Ref. [9]) are also shown for comparison. T_λ for the ^4He in porous gold experiment is 2.171 K because it is performed under applied pressure. The data for aerogel of 6% silica and for porous gold are shifted down by, respectively, 100 and 200 mJ/K cm^3 for clarity.

The temperature where the maximum in the heat capacity is found for samples II (5% silica) and IV (2% silica) are, respectively, within 400 and 300 μK of the values of T_c 's determined by ρ_s measurements on samples I (5% silica) and III (2% silica). Considering that these samples were grown in different laboratories and that samples II and IV are grown inside sintered silver grains, such agreements are satisfactory. The temperature of maximum heat capacity of sample V (0.5% silica) is 100 μK below the value of T_c as determined in ρ_s measurements. This is expected because the sinusoidal heat input results in a heat capacity peak that is temperature averaged. Because of the asymmetry in the shape of the ideal heat capacity peak, the “measured” peak position will be displaced to a lower temperature. Our analysis of the data, to be described below, indicates that a value of T_c that is on the order of 100 μK above the position of the apparent heat capacity maximum provides the best fit for data both below and above T_c . This means that, for sample V, the discrepancy (if any) in the T_c 's determined by heat capacity and ρ_s measurements is much less than 100 μK .

The heat capacity of ^4He in 5% aerogel as shown in Fig. 3 is in quantitative agreement with the results of 6% aerogel. In particular, there is no evidence of any singular feature below T_c . Interestingly, a divergent feature is found in the heat capacity of ^4He in porous gold. As the volume fraction of silica in aerogel is reduced below 5%, the heat capacity value increases dramatically and the singular contribution to the heat capacity becomes prominent below as well as above T_c . As is shown in Fig. 3, the heat capacity value at the peak increases by 25% and 50%, respectively, as the silica content is reduced from 5% to 2% and 0.5%.

The data are analyzed in the form [5,18,21]

$$C(t) = \frac{A'}{\alpha'} |t|^{-\alpha'} + B, \quad \text{for } t < 0, \text{ and}$$

$$C(t) = \frac{A}{\alpha} t^{-\alpha} + B, \quad \text{for } t > 0, \quad (3)$$

treating A , A' , α , and α' as independent fitting parameters. The data in reduced temperature range $-3 \times 10^{-3} < t < -5 \times 10^{-5}$ (40) and $5 \times 10^{-5} < t < 10^{-3}$ (45) for sample II (5% silica), $-3 \times 10^{-3} < t < -5 \times 10^{-5}$ (89) and $5 \times 10^{-5} < t < 10^{-3}$ (39) for sample IV (2% silica), and $-3 \times 10^{-3} < t < -5 \times 10^{-5}$ (40) and $5 \times 10^{-5} < t < 7 \times 10^{-4}$ (21) for sample V (0.5% silica) are used in the analysis. The numbers in parentheses are again the number of data points included in the analysis. The inner limit of the absolute value of the reduced temperature is dictated by the temperature oscillation of the calorimeter. For $T > T_c$, we did not include the data within 100 μK of T_λ in the analysis. Data in this range are more sensitive to an incorrect subtraction of the bulk signal. The best fit from a nonlinear least square procedure is found with the parameter values of

$$\alpha = -0.60 \pm 0.02, \quad \alpha' = -0.93 \pm 0.04,$$

for 5% aerogel, (4)

$$\alpha = -0.41 \pm 0.01, \quad \alpha' = -0.50 \pm 0.02,$$

for 2% aerogel, (5)

$$\alpha = -0.14 \pm 0.02, \quad \alpha' = -0.12 \pm 0.03,$$

for 0.5% aerogel. (6)

While the best fit values of α differ from α' for the 5% and 2% samples, in 0.5% aerogel the scaling law $\alpha = \alpha'$ is satisfied. Furthermore, the hyperscaling relation $2 - \alpha = d\nu = d\zeta$, violated in denser aerogels, is also satisfied ($\alpha = \alpha' = -0.13$, $\zeta = 0.72$) in the lightest aerogel.

Following Ref. [5], we repeat the analysis by imposing the $\alpha = \alpha'$ condition while following the same functional form as shown in Eq. (3). This constraint allows for the determination of the ratio A'/A . Such an analysis yields A'/A of 0.14 ± 0.12 (with $\alpha = \alpha' = -0.57 \pm 0.01$) for the 5% sample, 0.27 ± 0.06 (with $\alpha = \alpha' = -0.39 \pm 0.01$) for the 2% sample, and 0.50 ± 0.12 (with $\alpha = \alpha' = -0.13 \pm 0.02$) for aerogel with 0.5% silica.

To conclude, the superfluid density and heat capacity exponents, as well as the ratio A'/A , all show a smooth evolution towards the bulk ${}^4\text{He}$ value as the amount

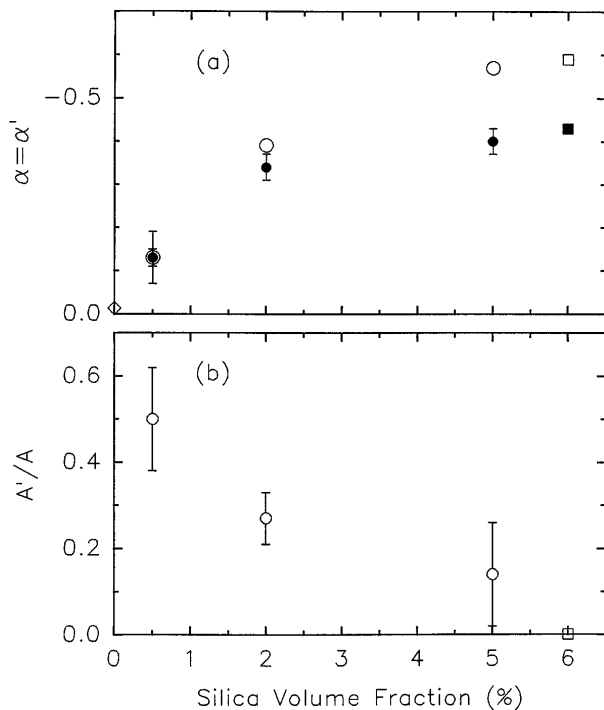


FIG. 4. (a) The values of $\alpha (= \alpha')$ in open symbols determined from heat capacity results are shown as a function of silica volume fraction in aerogel. Filled symbols are the values of α deduced from ζ through the hyperscaling relation ($2 - \alpha = d\zeta$). Values for 6% aerogel (squares, from Refs. [2,5]) and bulk ${}^4\text{He}$ (diamond, from Refs. [18,21]) are also shown. In 0.5% aerogel, the hyperscaling relation is satisfied. (b) The amplitude ratio for aerogels of different densities. The ratio A'/A for 6% aerogel is taken from Ref. [5]. For bulk ${}^4\text{He}$, $A'/A = 0.93$ (Ref. [18]).

of silica in aerogel is reduced below the 5% level. These evolutions are shown graphically in Fig. 4. The scaling law $\alpha = \alpha'$ and the hyperscaling relation, which appeared to be violated in denser aerogels, are satisfied in the lightest aerogel. With the results presented here and in earlier reports [1–5], the experimental information on the critical behavior of ${}^4\text{He}$ in aerogel is reasonably complete. These results pose a challenge for further theoretical investigation.

We thank Lawrence Hrubesh for growing aerogel samples I and III used in this experiment, and John Reppy, Gane Wong, and Geoff Zassenhaus for making available the 6% aerogel heat capacity data. This work is supported by NSF under Grants No. DMR-9311918 and No. DMR-9630736.

*Present address: Department of Electrical Engineering, Princeton University, Princeton, NJ 08544.

†Present address: Department of Physics and Astronomy, University of New Mexico, Albuquerque, NM 87131.

‡Present address: Department of Physics, Amherst College, Amherst, MA 01002.

§Present address: Department of Physics and Astronomy, University of Delaware, Newark, DE 19716.

- [1] M. Chan, N. Mulders, and J. Reppy, *Phys. Today* **49**, No. 8, 30 (1996).
- [2] M. H. W. Chan *et al.*, *Phys. Rev. Lett.* **61**, 1950 (1988).
- [3] G. K. S. Wong *et al.*, *Phys. Rev. Lett.* **65**, 2410 (1990); *Phys. Rev. B* **48**, 3858 (1993).
- [4] N. Mulders *et al.*, *Phys. Rev. Lett.* **67**, 695 (1991).
- [5] M. Larson, N. Mulders, and G. Ahlers, *Phys. Rev. Lett.* **68**, 3896 (1992); M. Larson *et al.*, *J. Low Temp. Phys.* **89**, 79 (1992).
- [6] J. Fricke, *Sci. Am.* **258**, No. 5, 92 (1988).
- [7] G. C. Ruben, L. W. Hrubesh, and T. M. Tillotson, *J. Non-Cryst. Solids* **186**, 209 (1995).
- [8] L. S. Goldner, N. Mulders, and G. Ahlers, *J. Low Temp. Phys.* **93**, 131 (1993).
- [9] J. Yoon and M. H. W. Chan, *Phys. Rev. Lett.* **78**, 4801 (1997).
- [10] A. B. Harris, *J. Phys. C* **7**, 1671 (1974); D. S. Fisher, G. M. Grinstein, and A. Khurana, *Phys. Today* **41**, No. 12, 56 (1988).
- [11] A. Weinrib and B. I. Halperin, *Phys. Rev. B* **27**, 413 (1983).
- [12] K. Moon and S. M. Girvin, *Phys. Rev. Lett.* **75**, 1328 (1995).
- [13] R. C. Newmann and K. Sieradzki, *Science* **263**, 1708 (1994).
- [14] P. Levitz *et al.*, *J. Chem. Phys.* **95**, 6151 (1991).
- [15] R. Vacher *et al.*, *Phys. Rev. B* **37**, 6500 (1988).
- [16] B. D. Josephson, *Phys. Lett.* **21**, 608 (1966).
- [17] M. E. Fisher, M. N. Barber, and D. Jasnow, *Phys. Rev. A* **8**, 1111 (1973).
- [18] G. Ahlers, *Phys. Rev. A* **3**, 696 (1971).
- [19] N. Mulders and L. Lurio (private communication).
- [20] P. F. Sullivan and G. Seidel, *Phys. Rev.* **173**, 679 (1968).
- [21] J. A. Lipa *et al.*, *Phys. Rev. Lett.* **76**, 944 (1996).